Chirp Characterization of External Modulators With Finite Extinction Ratio Using Linear Optical Sampling

Tasshi Dennis and Paul A. Williams

***Abstract*—We demonstrate a network monitoring technique for the frequency chirping of external modulators based on linear optical sampling. We present α-parameter waveforms of digital data modulation from simultaneously measured amplitude and phase. Digital data modulation was compared to sinusoidal modulation to demonstrate the measurement capabilities. The high sensitivity of our technique was used to resolve the detailed impact of a 23-dB extinction ratio on the chirp of a Mach–Zehnder modulator. Unlike some previous methods, a monochromator or optical fiber with known dispersion are not required.**

***Index Terms*—Chirp, coherent detection, linear optical sampling (LOS), optical network monitoring.**

I. Introduction

FUTURE optical networks will require a sophisticated level of reconfigurability to adapt to dynamic traffic needs and to mitigate system impairments. This approach necessitates real-time performance monitoring of the system parameters, including modulator chirp as considered here. For example, chromatic dispersion of optical fiber is a physical impairment that can change with environmental effects and path reconfiguration. Residual phase modulation of intensity modulators can be used advantageously to provide an adjustable amount of pulse compression to offset chromatic dispersion [1]. Known as chirp, this property can arise in external Mach–Zehnder modulators (MZMs) from unbalanced modulation indices or drive voltages in the two waveguides, and from a finite interferometer extinction ratio [2]. Modulators can be designed to exploit these chirp dependencies to allow dynamic dispersion compensation.

Popular laboratory techniques for characterizing the chirp of external modulators include optical spectrum analysis of sidebands [3], [4], and electrical spectrum analysis of fiber response [5], [6]. More appropriate to impairment monitoring are techniques that measure the dynamic chirp of data modulated signals by use of monochromators [7] and arrayed waveguide gratings [8]. In this work, we present a coherent technique based on linear optical sampling (LOS) of modulated data using a quadrature receiver, which follows the preliminary work of [9].

The chirp of a modulator can be fully described by the α-parameter [10], which is a unitless quantity defined as

$$\alpha = 2I\frac{d\varphi/dt}{dI/dt} \tag{1}$$

Manuscript received October 30, 2009; revised December 23, 2009; accepted January 07, 2010. Date of publication February 22, 2010; date of current version April 09, 2010.

The authors are with the National Institute of Standards and Technology, Boulder, CO 80305 USA (e-mail: tasshi@boulder.nist.gov; pwilliam@boulder.nist.gov).

Digital Object Identifier 10.1109/LPT.2010.2043356

where I is the modulated optical intensity and φ is the phase. As demonstrated in [7], α can be evaluated from measurements of time-dependent intensity and phase by use of (1). For an MZM with two electrodes and driving voltages V_1 and V_2, modulation indices η_1 and η_2, dc bias voltage V_b, and switching voltage V_π, the α-parameter following [6] and [11] is

$$\alpha = \frac{\eta_2 V_2 + \eta_1 V_1}{\eta_2 V_2 - \eta_1 V_1}\cot\left(\frac{\pi}{2V_\pi}(V_1 + V_2 + V_b)\right). \tag{2}$$

For a given modulator, the bias voltage V_b is a convenient way to externally vary the α-parameter. By definition, the chirp parameter $\mathcal{V}$ is the front half of (2),

$$\mathcal{V} = \frac{\eta_2 V_2 + \eta_1 V_1}{\eta_2 V_2 - \eta_1 V_1} \tag{3}$$

and is the small-signal value of the α-parameter at quadrature bias. It is apparent from (3) that $\mathcal{V}$ can be adjusted either by changing the balance between the drive voltages V_1 and V_2 or the modulation indices η_1 and η_2. While η_1 and η_2 are usually fixed during manufacture, dual-electrode modulators allow the drive voltages to be varied independently.

Frequency chirping can also arise from a finite dc extinction ratio δ, resulting from asymmetric splitting in the Y-branch waveguides of an MZM. Here we model the asymmetry with normalized coefficients $R^{1/2}$ and $(1-R)^{1/2}$ for the recombined electric fields at the modulator output, which are related to the extinction by

$$R = \frac{1}{2} \pm \frac{\sqrt{\delta}}{1+\delta}. \tag{4}$$

Following the development in [2], and assuming small-signal push–pull ($V_1 = -V_2$) sinusoidal modulation, the expression for α is

$$\alpha = \frac{R\eta_1 + (1-R)\eta_2 + \sqrt{R}\sqrt{1-R}(\eta_1+\eta_2)\cos\left(\frac{\pi V_b}{V_\pi}\right)}{-\sqrt{R}\sqrt{1-R}(\eta_1-\eta_2)\sin\left(\frac{\pi V_b}{V_\pi}\right)}. \tag{5}$$

At quadrature bias, this expression gives the extinction ratio dependent chirp parameter as

$$\mathcal{V} = \frac{(R\eta_1 + (1-R)\eta_2)}{\sqrt{R}\sqrt{1-R}(\eta_1-\eta_2)} \tag{6}$$

which is equivalent to expressions in [2] and [4].

In this work, we use LOS to make simultaneous measurements of time-dependent intensity and phase to allow α to be evaluated from (1). Following the approach of [6], we map the α-parameter as a function of bias voltage to demonstrate the

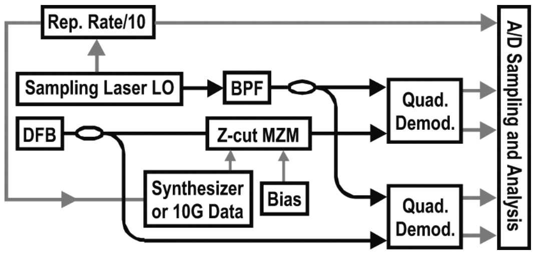

Fig. 1. LOS system configured for measuring modulator chirp: BPF: optical bandpass filter. Grey paths are electrical and black paths are optical.

measurement range, and in turn to examine the effect of extinction ratio. The application to impairment monitoring is demonstrated by comparing α measured from 10-Gb/s data modulation to that from sinusoidal modulation.

II. Experiment and Results

Our chirp measurements were carried out by use of the LOS system shown in Fig. 1. LOS uses a short-pulsed laser as a local oscillator (LO) to interferometrically down-sample a modulated optical signal by use of a quadrature demodulator [12]. This technique measures the full complex electric field of an optical signal with low-bandwidth detection, and through equivalent-time sampling can measure complex high-speed waveforms. Our sampling laser was a 100-MHz fiber frequency comb shaped by a 0.5-nm bandpass filter to yield 6.2-ps pulses. We created a 10-MHz synchronization frequency by dividing the detected comb repetition rate by 10. The distributed-feedback (DFB) laser at 1558 nm was intensity modulated with a Z-cut lithium-niobate MZM. Light from the DFB was measured before and after modulation to perform phase referencing [12], which isolated the residual phase modulation from the drift of the DFB carrier. The intensity was obtained from the amplitude of a single demodulator. The outputs from four 350-MHz balanced demodulator detectors were simultaneously sampled and processed offline to reconstruct the electric field of the data signal.

Fig. 2 presents a typical measurement when the modulator is biased at quadrature, showing the time-domain intensity, phase, and calculated α-parameter for a repeated 16-bit data sequence at 10 Gb/s. Our 1-ms total measurement duration allowed the sequence to be recorded over 60 times, which enabled us to average the 16-bit sequence for an $\sim$8 times noise reduction. This averaging and additional low-pass digital filtering of the intensity and phase were critical to reducing point-to-point noise in the calculated derivatives. The discontinuities in the α-parameter shown in Fig. 2(c) are from division by zero occurring each time the intensity slope was zero. At these points the calculated α was as large as ± 500 and extended well off the limited plot range. The operational α-parameter of the modulator was determined as the median of the complete α waveform [7], which is fairly insensitive to the discontinuities. For Fig. 2(c) the median α was 0.75, as indicated, and is consistent with a Z-cut modulator at quadrature.

The α-parameter characteristic was measured by use of sinusoidal modulation at 5 GHz while slowly stepping the bias voltage of the modulator, as shown with dots in Fig. 3(a). The solid line is a plot of (2) with $V_\pi = 2.35$ V and $\mathcal{V} = 0.75$, demonstrating good agreement over a 4π range of bias control.

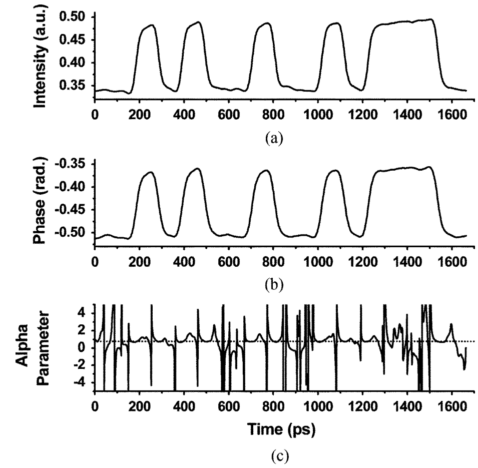

Fig. 2. Measurements of 16-bit data modulation, consisting of (a) intensity , (b) phase, and (c) calculated α-parameter waveforms. The limited plot range in (c) shows detail but clips discontinuities; the dotted line is the median α.

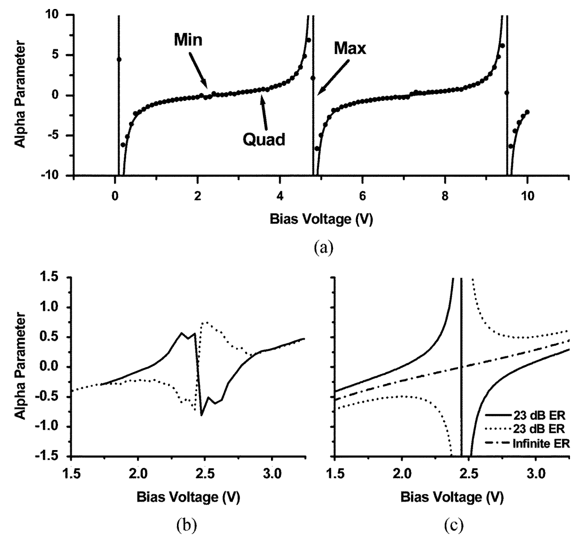

Fig. 3. Chirp characterization versus bias voltage: in (a) a broad scan (dotted line) is compared to theory (solid line), in (b) detailed measurements around minimum transmission, and in (c) theoretical modeling of finite extinction ratio.

At the minimum bias positions near 2.5 and 7.2 V the measured α curve shows a slight irregularity. Fig. 3(b) presents two detailed measurements of this region by use of small bias steps, small sinusoidal modulation, and the averaging of ten α measurements per data point. The two curves were measured one after the other, yet they deviate uniquely from the expected cotangent behavior. To compare with theory, Fig. 3(c) shows plots of (5) calculated based on a measured extinction ratio of 23 dB. An infinite extinction curve is also shown. The two curves shown for 23-dB extinction correspond to equivalent conditions in which $R = 0.43$ and $R = 0.57$. We believe this parity results from the ambiguity in distinguishing the two Mach–Zehnder arms of the modulator and defining whether the phase of one leads or lags the other. In any case, the measurements of Fig. 3(b) are consistent with a modulator having a very large yet finite extinction ratio.

While the characterization of a modulator with a sinusoidal signal gives excellent results, the use of digital data modulation (Fig. 2) would be much more practical for monitoring of chirp in a live network. To test the limits of this approach, we

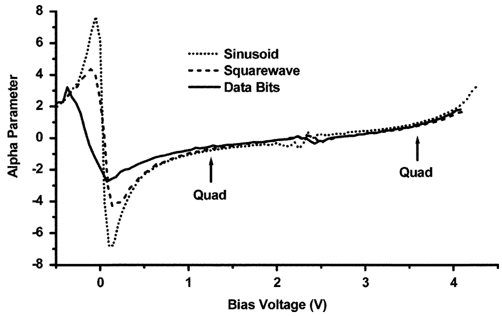

Fig. 4. Comparison of chirp measurements using sinusoidal, square-wave, and digital data modulation.

compared measurements of the α-parameter from 5-GHz sinusoidal, 5-GHz square-wave, and 10-Gb/s digital data modulation. The comparison is difficult to make because the time interval required to measure all three curves was sufficient to allow bias drift. Fig. 4 presents the results, which include slight lateral shifts of the data ($\leq$0.1 V) to quantitatively align the apparent zero crossings at minimum bias. The curves agree well over much of the measurement range, but show increasing differences as the α-parameters approach the maximum bias near 0 V. Our modeling suggested that this distortion resulted from the digital low-pass filtering, which had a greater impact on square and digital data waveforms owing to their higher frequency content. The distortion was greatest near the maximum bias point because of the nonlinearity of the modulation. By increasing the waveform averaging with a measurement longer than 1 ms, it should be possible to reduce the low-pass filtering and the measurement distortion. However, doing so would also allow more time for bias drift.

At the more significant quadrature bias points, indicated at 1.2 and 3.6 V in Fig. 4, the average difference in α between sinusoidal and digital data measurements was only 0.19. This quantitative comparison is not rigorous because only moderate averaging was used and the bias was drifting. A bias controller or quadrature locking circuit would have eliminated this drift, and would be integral to a chirped network transmitter. A more sophisticated waveform analysis could also yield better results, such as excluding the discontinuities of Fig. 2(c) that do not contribute meaningful information to the median α. The promising results in Fig. 4 at quadrature bias indicate that with optimization, LOS could become a valuable monitoring tool.

III. Discussion and Conclusion

The amplitude of the electrical drive signal is an important consideration in the characterization of the α-parameter [7]. A larger drive signal will improve the signal-to-noise ratio but can wash out α-parameter details, especially near the maximum and minimum bias points. These points are difficult to measure because the modulation is highly nonlinear. Fig. 2(c) illustrates how the time-domain α-parameter swings about the α curve for a drive voltage of $\pm$0.4 V while giving a median α of 0.75. In Fig. 3(a) the measurable limit for a drive of $\pm$0.5 V was a median value of α no larger than $\pm$7.

The deviation of the α-parameter in Fig. 3(b) is relevant to implementations of phase-shift-keying modulation that switch across minimum bias because of corresponding distortions to the constellation diagram. The modulator we measured had a significant range in extinction ratio (14–30 dB), depending on the particular minimum, so it was important that it be characterized under precise operating conditions. Fig. 3(c) shows that the deviation from perfect extinction extends to other bias points: at quadrature the deviation of α is 0.15.

Phase referencing was necessary in this work to remove carrier phase drift. However, at a remote network receiver the unmodulated carrier is generally unavailable, so carrier phase estimation would be necessary. Such estimation techniques require either real-time sampling or much faster equivalent time sampling. Our use of 100-MHz equivalent time sampling required a repeated data sequence, which also enabled averaging. In a real network this sequence could come from a test pattern or a recurring packet header.

We have demonstrated a sensitive chirp monitoring technique appropriate for digital data modulation without the need for a spectrometer. The technique allowed us to study the operation of a modulator and the measurement process. This work has revealed a number of topics for future consideration, including the impact of drive amplitude, digital filtering, bias drift, and signal format.

References

[1] S. K. Kim, O. Mizuhara, Y. K. Park, L. D. Tzeng, Y. S. Kim, and J. Jeong, "Theoretical and experimental study of 10 Gb/s transmission performance using $1.55\ \mu$m LiNbO3-based transmitters with adjustable extinction ratio and chirp," *J. Lightw. Technol.*, vol. 17, no. 8, pp. 1320–1325, Aug. 1999.

[2] H. Kim and A. H. Gnauck, "Chirp characteristics of dual-drive Mach–Zehnder modulator with a finite DC extinction ratio," *IEEE Photon. Technol. Lett.*, vol. 14, no. 3, pp. 298–300, Mar. 2002.

[3] M. Suzuki, Y. Noda, Y. Kushiro, and S. Akiba, "Dynamic spectral width of an InGaAsP/InP electroabsorption light modulator under high-frequency large-signal modulation," *Electron. Lett.*, vol. 22, pp. 312–313, Mar. 1986.

[4] N. Courjal, J. M. Dudley, and H. Porte, "Extinction-ratio-independent method for chirp measurement of Mach–Zehnder modulators," *Opt. Express*, vol. 12, pp. 442–448, Feb. 2004.

[5] F. Devaux, Y. Sorel, and J. F. Kerdiles, "Simple measurement of fiber dispersion and of chirp parameter of intensity modulated light emitter," *J. Lightw. Technol.*, vol. 11, no. 12, pp. 1937–1940, Dec. 1993.

[6] M. Schiess and H. Carldén, "Evaluation of the chirp parameter of a Mach–Zehnder intensity modulator," *Electron. Lett.*, vol. 30, pp. 1524–1525, Sep. 1994.

[7] J. Jeong and Y. K. Park, "Accurate determination of transient chirp parameter in high speed digital lightwave transmitters," *Electron. Lett.*, vol. 33, pp. 605–606, Mar. 1997.

[8] R. Monnard, C. R. Doerr, and C. R. Giles, "Real-time dynamic chirp measurements of optical signal," in *Proc. OFC 1998*, San Jose, CA, Feb. 22–27, 1998, pp. 120–121.

[9] I. Fatadin and D. Ives, "Amplitude and phase measurements of optical signals using a coherent technique," in *Proc. OFMC 2009*, Teddington, UK, Sep. 16–18, , pp. 25–28.

[10] F. Koyama and K. Iga, "Frequency chirping in external modulators," *J. Lightw. Technol.*, vol. 6, no. 1, pp. 87–93, Jan. 1988.

[11] A. Djupsjöbacka, "Residual chirp in integrated-optic modulators," *IEEE Photon. Technol. Lett.*, vol. 4, no. 1, pp. 41–43, Jan. 1992.

[12] P. A. Williams, T. Dennis, I. Coddington, W. C. Swann, and N. R. Newbury, "Vector signal characterization of high-speed optical components by use of linear optical sampling with milliradian resolution," *IEEE Photon. Technol. Lett.*, vol. 20, no. 23, pp. 2007–2009, Dec. 1, 2008.